



## Workshop on Limits to Diversity Assembly | (SMR 3594)

19 Jan 2021 - 21 Jan 2021  
Virtual, Virtual, Italy

---

### **P01 - ADIAHA Monday Sunday**

MAPPING BIODIVERSITY VARIABILITY IN THE ECOSYSTEM-NEXUS OF TROPICAL SOILS

### **P02 - DE GOËR DE HERVE Mathieu Yves Gregoire**

Using discrete-event models to predict the non-reproducible outcomes of a top-down community assembly experiment.

### **P03 - DE OLIVEIRA SUDBRACK Vitor**

Population dynamics in highly fragmented landscapes

### **P04 - LERNER Irina**

Structuring and Optimization of an individual based model

### **P05 - NUNES De Araujo Dornelas Vivian**

Impact of the landscape heterogeneity on the spatial organization of a single-species population

### **P06 - PHAM Minh Tuan**

Predicting collapse of adaptive networked systems without knowing the network

### **P07 - PRINCEPE Debora**

Patterns of speciation and diversification in a model with selection over mito-nuclear compatibility



## MAPPING BIODIVERSITY VARIABILITY IN THE ECOSYSTEM-NEXUS OF TROPICAL SOILS



**M. S. ADIAHA**

*Academic Researcher/Scientist*

Nigeria Institute of Soil Science (NISS)

Google Scholar: <https://scholar.google.com/citations?user=4BIIXPIAAAAJ&hl=en>



## Introduction

It is no more news that the deterioration of our mother Earth has resulted in many hardships faced in many lands of the world. Research statistics has shown that about 80% of the environmental problems faced in Asia, especially the loss of soil biodiversity results from deforestation. Africa has been intensely affected by the hazards of climate change at a rate of more than 50%, also Near East and North Africa has recorded more than 48% loss of her biodiversity in soils due to habitat alteration and loss. This list is inexhaustive and heart-broken, presenting a view that if sustainable remediation is not taken then we will have more malnourished and sick people in years to come, our environment will be more polluted and toxic, our water system will become more and more difficult to remediate, there could be increase in local, national and international conflict among other unforeseen unpleasant happenings. To contribute as a modality towards solving this problem.

## Objective and Method of the Study

this study investigated the current biodiversity variability in the ecosystem-nexus of soils. The study took place within the University of Abuja landmass. Spatial and temporal data were collected on earth-system properties, were analysis and simulations were done. The Area was model and interpolated to find hot spots with grave threat. Descriptive statistics was applied in the study.

*Keywords: Mapping Biodiversity; Variability; Ecosystem-Nexus; Tropical Soils; Vetiver Grass Technology*

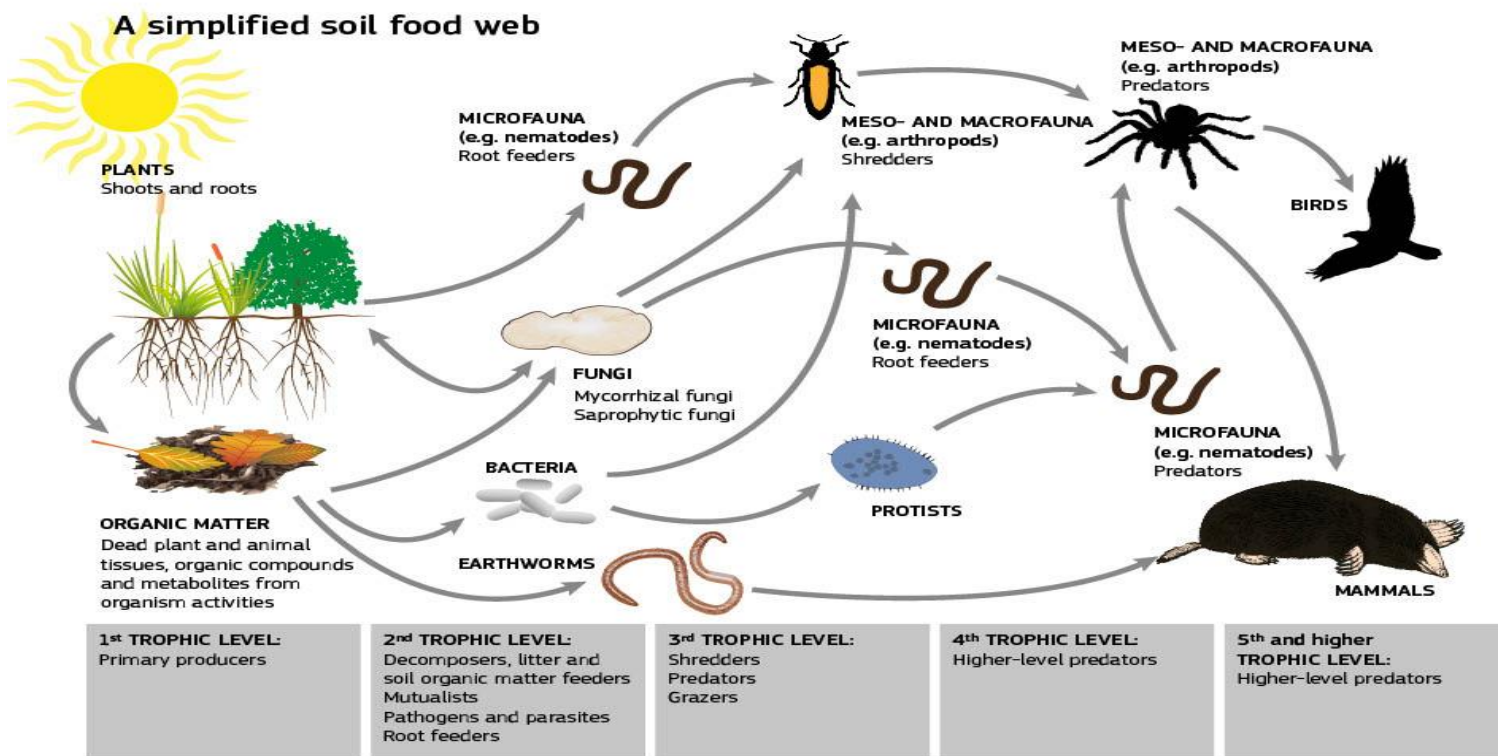
### Typical numbers of soil organisms in healthy ecosystem

|            |  | Agricultural soils   | Prairie soils  | Forest soils  |
|------------|--|--|--|---|
| Bacteria   | Per teaspoon of soil (1 gram dry)                        | 100 million to 1 billion   | 100 million to 1 billion   | 100 million to 1 billion  |
| Fungi      |  | Several yards<br>(dominated by vesicular-arbuscular mycorrhizal fungi)             | Tens to hundreds of yards<br>(dominated by vesicular-arbuscular mycorrhizal fungi) | Several hundreds of yards in deciduous forests<br>One to forty miles in coniferous forests (dominated by ectomycorrhizal fungi) |
| Protozoa   |  | Several thousand flagellates and amoebae, one hundred to several hundred ciliates  | Several thousand and amoebae, one hundred to several hundred ciliates              | Several hundred thousand amoebae, fewer flagellates   |
| Nematodes  |  | Ten to twenty bacterial-feeders<br>A few fungal-feeders<br>Few predatory nematodes | Tens to several hundred  | Several hundred bacterial- and fungal-feeders<br>Many predatory nematodes   |
| Arthropods |  | Per square foot  | Up to one hundred  | Five hundred to two thousand  |
| Earthworms | Five to thirty<br>More in soils with high organic matter |  | Ten to fifty<br>Arid or semi-arid areas may have none                              | Ten to fifty in deciduous woodlands<br>Very few in coniferous forests   |

Note: 1 foot = 0.3048 m; 1 yard = 0.9144 m; 1 mile = 1.609344 km.

Source: country report of the United States of America. <https://www.nrcs>

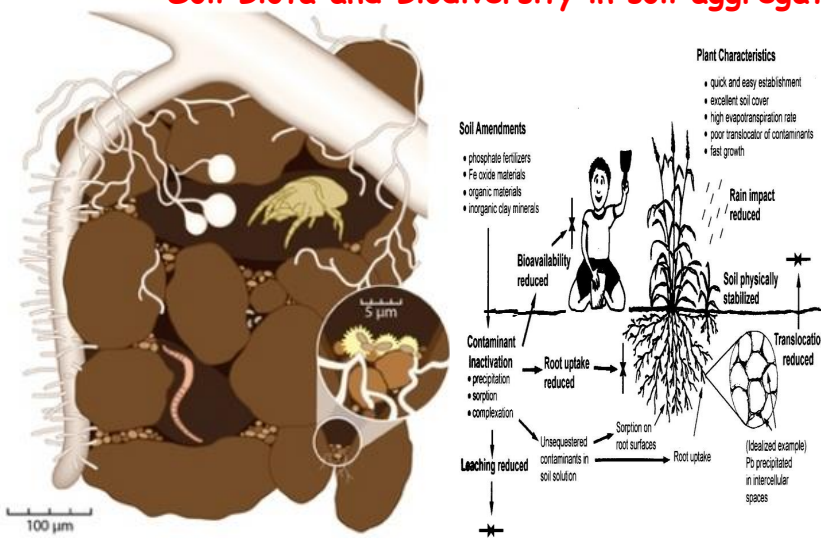
## The Soil Living System



Source: State of the World's Biodiversity for FAO (2016)



## Soil Biota and Biodiversity in soil aggregate

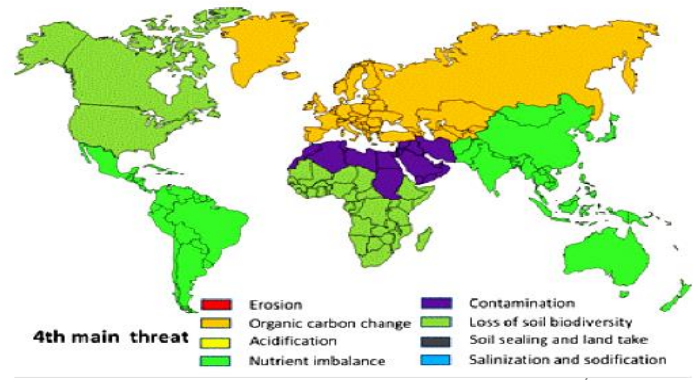
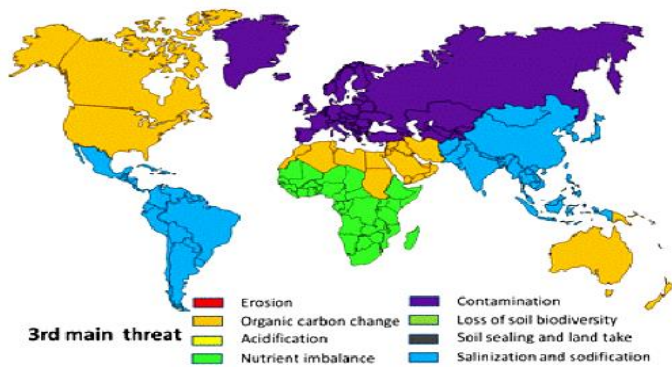
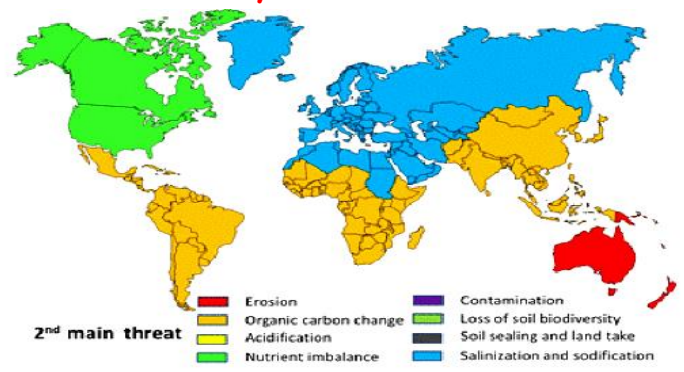
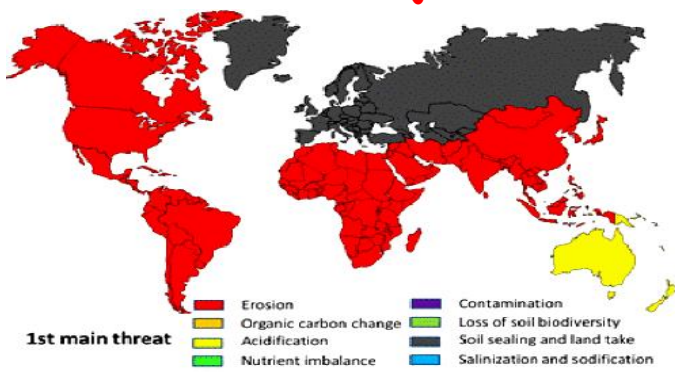


A soil aggregate or ped is a naturally formed assemblage of sand, silt, clay, organic matter, root hairs, macro and micro organisms and their secretions, and resulting pores.



Source: State of the World's Biodiversity for FAO (2016)

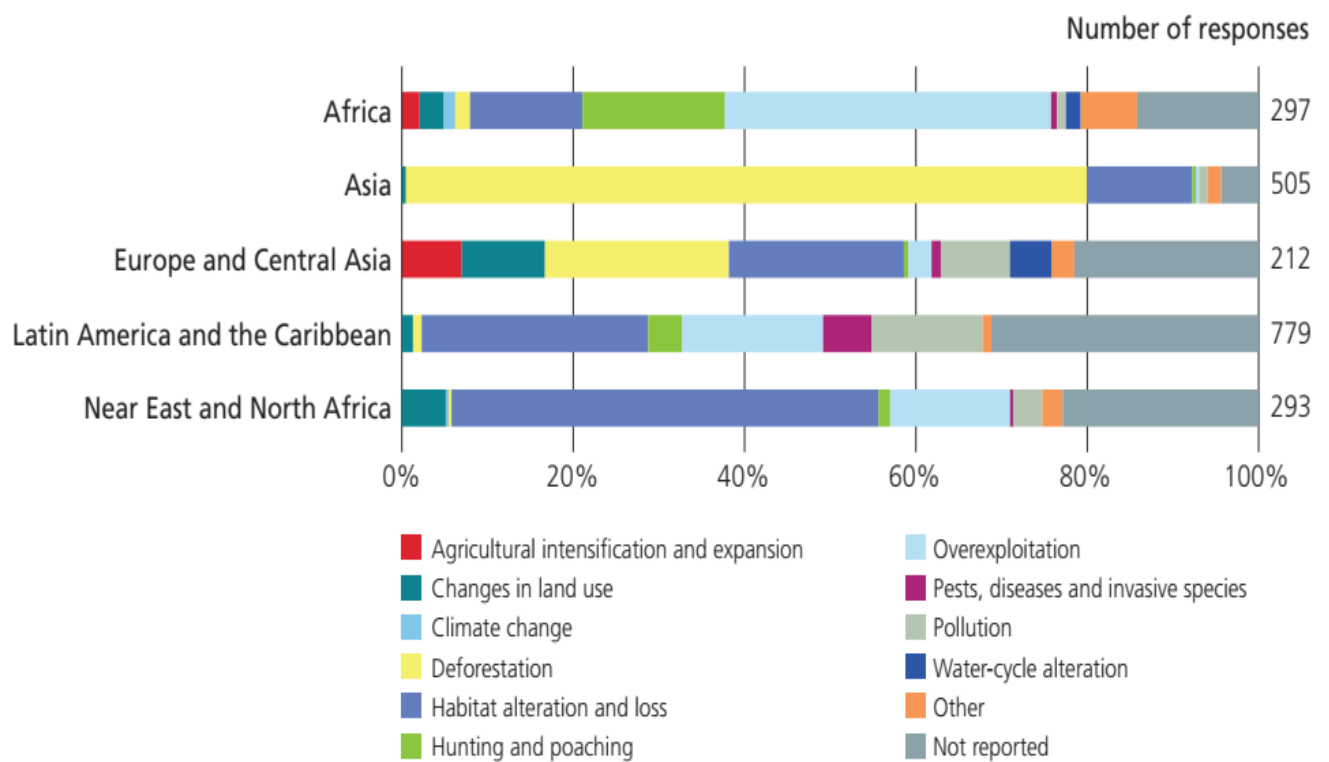
## Major Threat to soil health and Biodiversity



Source: Modified from the State of the World's Biodiversity for FAO

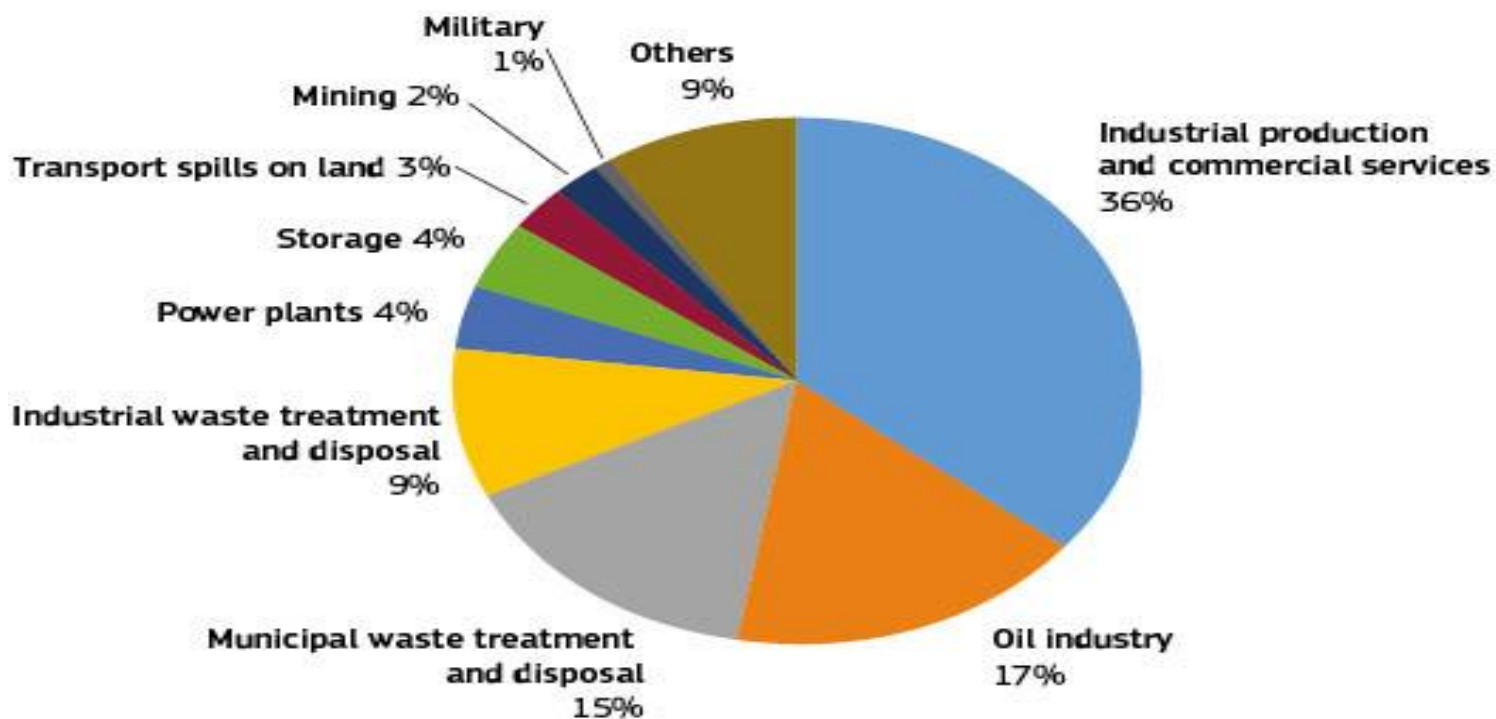


## Reported threats contributing to Soil biodiversity Decline



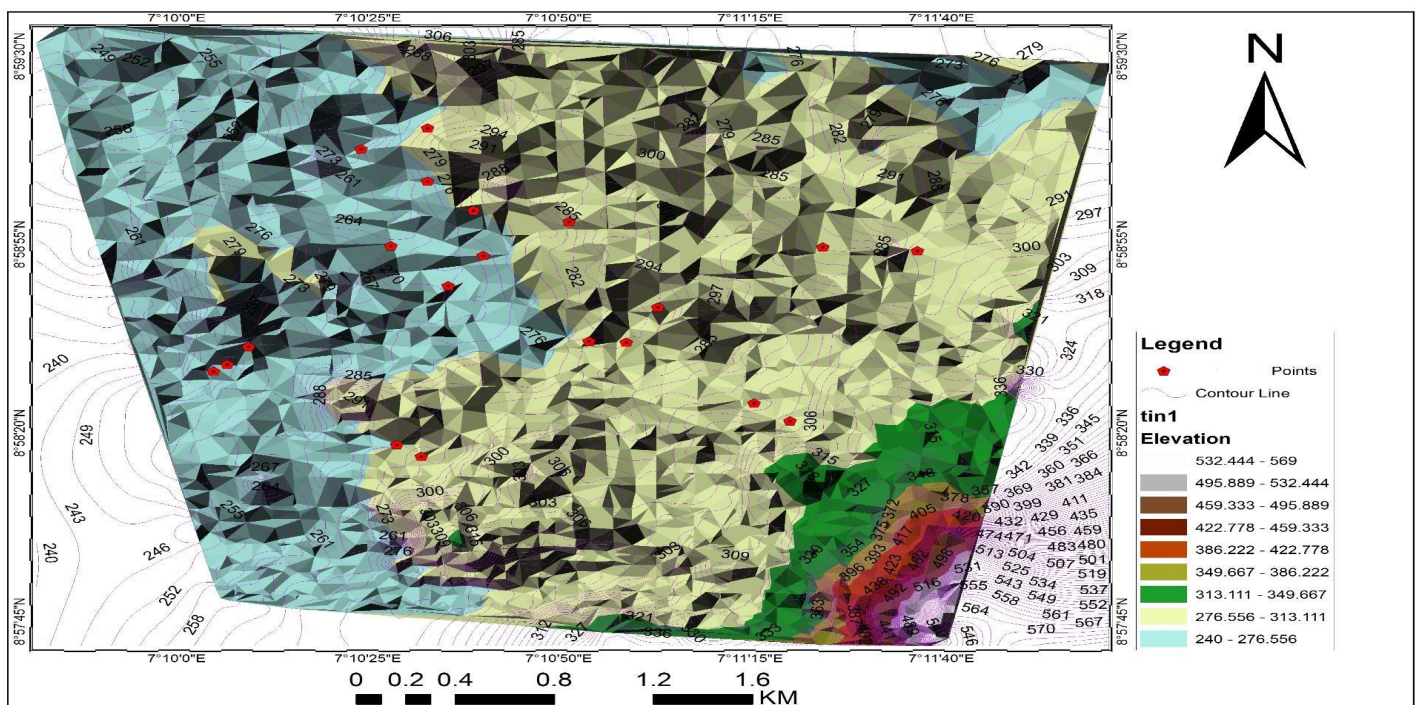
Source: Modified from the State of the World's Biodiversity for FAO

### Human Threat to Soil Health and Biodiversity



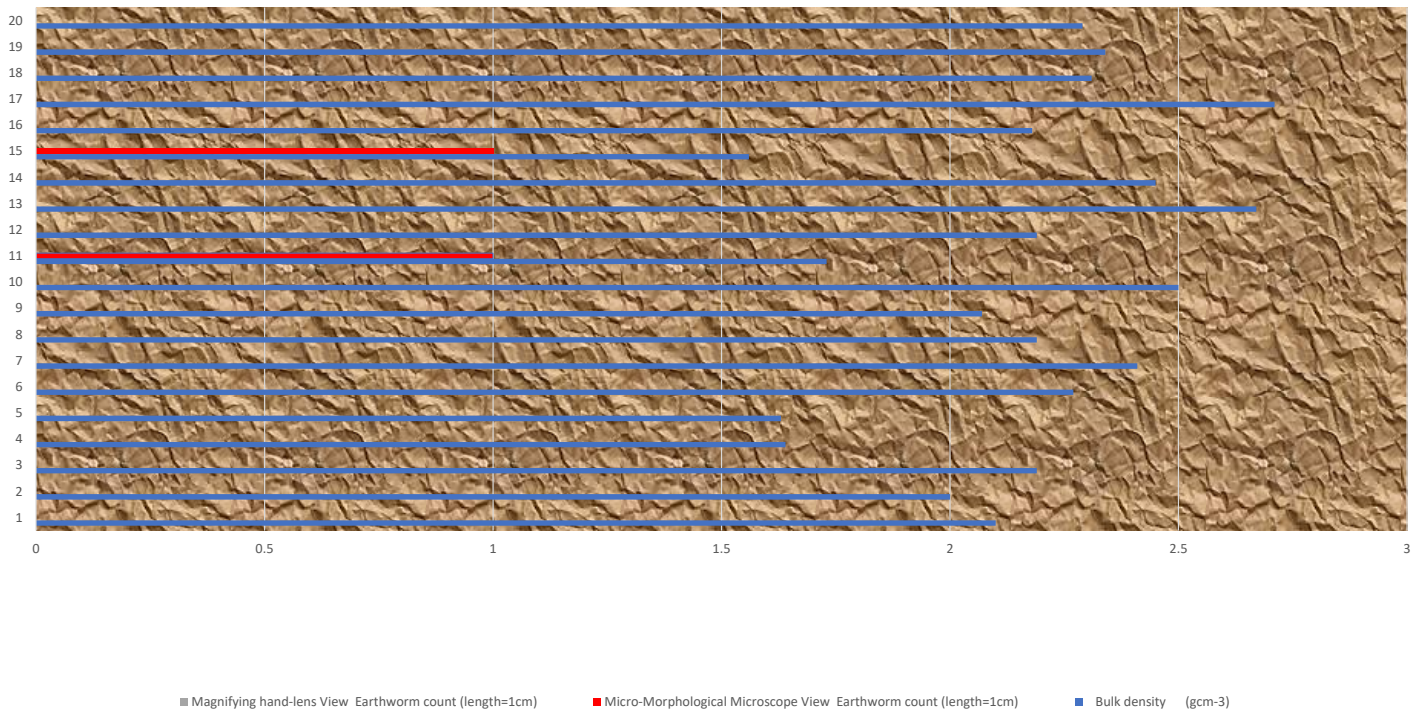
Source: Modification and Visualization was done from the data of State of the World's Biodiversity for FAO (2016)

Result: Mapping Soil Biodiversity Distribution in Soils of University of Abuja

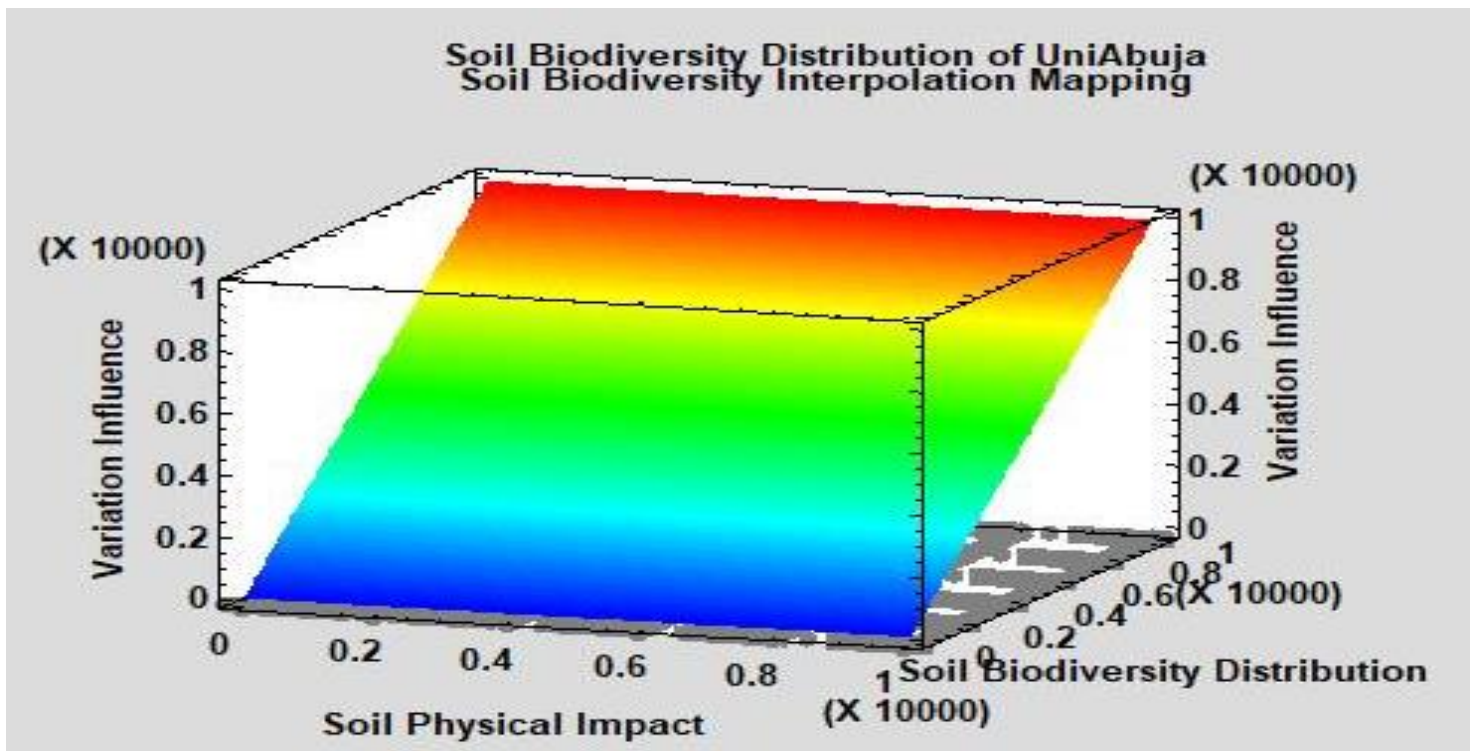


# Result

## Impact of compaction on Soil Biodiversity in Soils of Nigeria

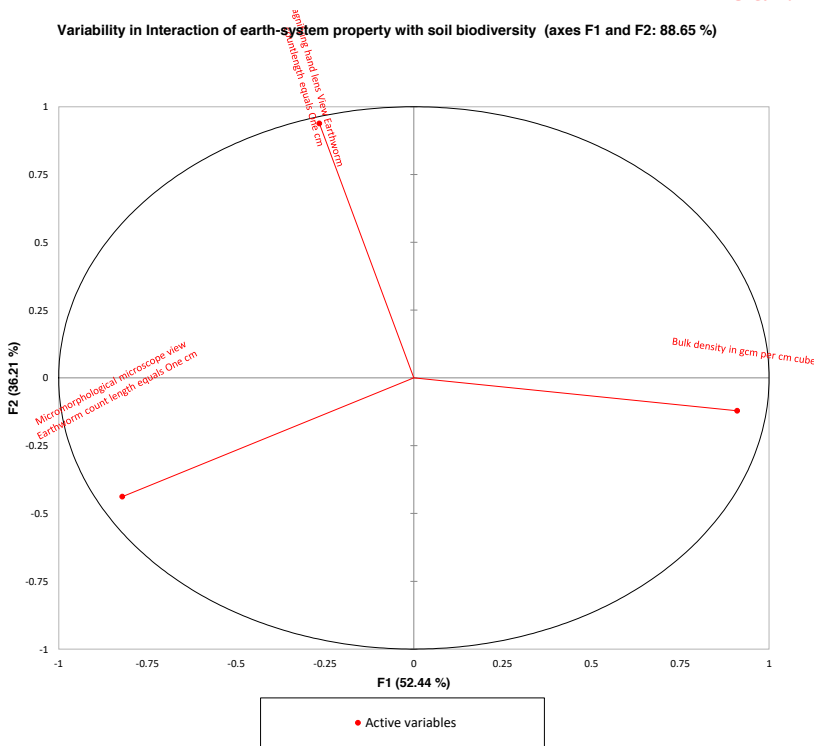


## Result: Area Interpolation

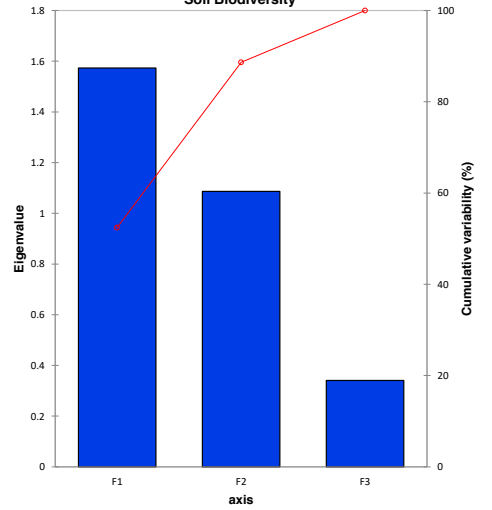


# Result

Variability in Interaction of earth-system property with soil biodiversity (axes F1 and F2: 88.65 %)



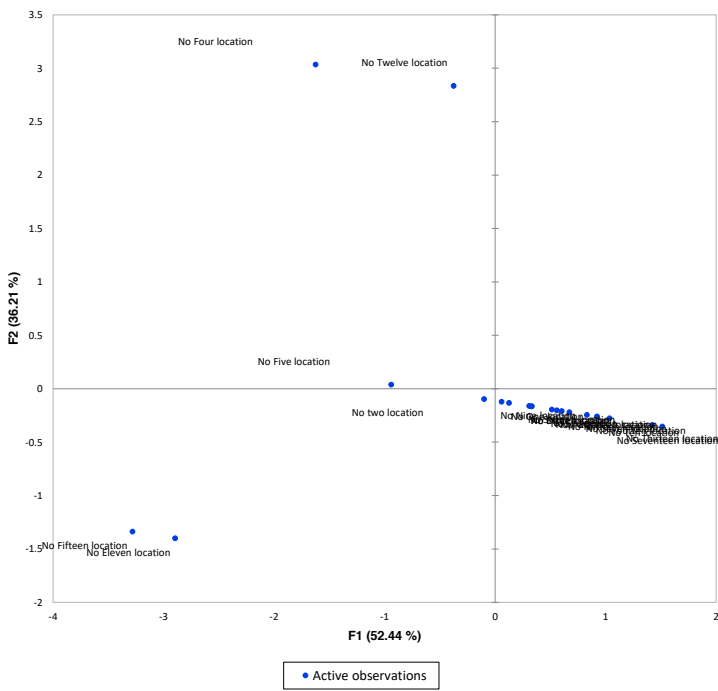
Variability Rating Influence on Earth-system properties and Soil Biodiversity





## Soil Biodiversity variation

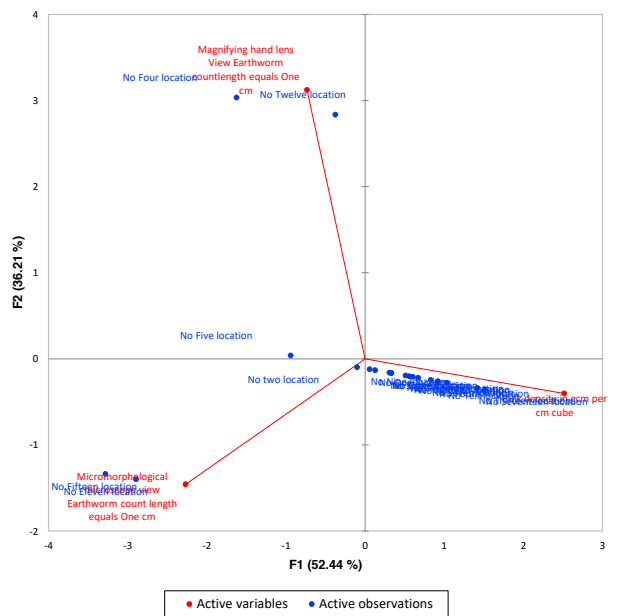
Soil Biodiversity concentration at site with good soil properties (axes F1 and F2: 88.65%)



## Result

### Bd Influence on soil Biodiversity

Bd influence on soil Biodiversity (axes F1 and F2: 88.65%)



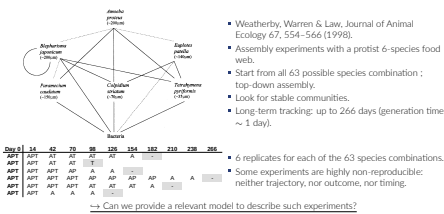
### **Main Findings/Conclusion and Recommendation**

Results indicated that the soils of the study area are compacted and hence unfit to support sustainable survival of the living entities within the soil system, with soil Bulk density value range at  $2.1\text{gcm}^{-3}$  -  $2.71\text{gcm}^{-3}$ . Geotechnical and geomorphological evaluation and interactions revealed only two (2) points having earthworm length of 1 cm which presented a view that the soils spore is too tight to enable sustainable flourishing of below and above ground biodiversity in the sites investigated. Hence ecological tool like the use of Vetiver Grass Technology was recommended for the study area environmental regeneration and for healing the soils impediment

## Using discrete-event models to predict the non-reproducible outcomes of a top-down community assembly experiment.

Mathieu de Goër de Herve, Colin Thomas, Maximilien Cosme, Boris Flotterer, Franck Pommereau, Philip Warren, Richard Law, Cédric Gaucherel  
 AMAP laboratory, Montpellier, France.

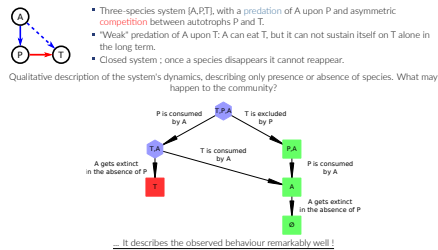
### The Weatherby 1998 experiments



### Model choice

- **Deterministic, averaging** approach.  
 → ... What's the average of communities with different compositions?  
 → complex model, relying on many parameters...
- **Full probabilistic** approach.  
 → ... Some of which can't really be measured (e.g. resources).  
 → ... And not enough replicates to measure probability distributions in a meaningful way!
- **Qualitative, possibilistic** approach.  
 → Can we get significant information without numbers?

### Qualitative model for the APT experiment

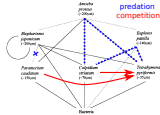


### A discrete-event model.

- **Stochian** states: absence (+) / presence (-) of components.
  - **Events** that modify the state of the system (appearance/disappearance of a species) lead to **transitions** between the states.
  - The interactions between components are translated as the events they can cause: conditions → state modifications.  
 E.g. predation of A upon P ⇒ {A+ → P-, P- → A-}
  - For each possible state, we compute which events are allowed and which transitions they lead to, and draw the **state space**.
  - **Asynchrony** of the model: describes different possible timelines, one event at a time.
  - **Possibilistic** model: we compute all possible trajectories and futures for the system.
- Gaucherel & Pommereau, *Methods in Ecology and Evolution* 10, 1615–1627 (2019).

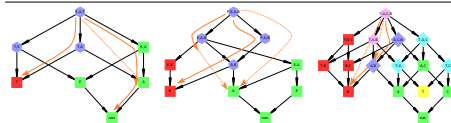
### Complete model of the network

- Three types of interactions: competition, predation, weak predation.
- We use the results of experiments starting from pairs of species to refine the model and determine the interactions within the system.
- These experiments lead to a model slightly different from the trophic network proposed in the paper.

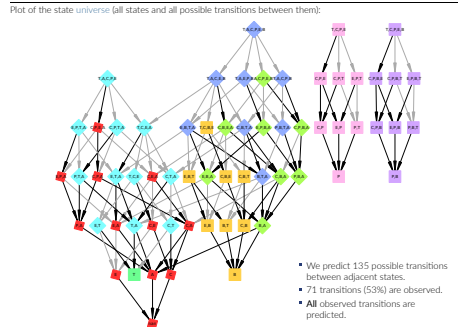


- The hypotheses we made for our model were actually justified in a later paper from the same team (Law et al, *Oikos* 88 (2000))
- Addition of rule C+ → C-, as C seems to sometimes disappear alone.

### A few examples of predictions and realizations



### State universe



### Model-data comparison

- We do NOT expect to observe all trajectories, for two reasons:
- Statistics: some events are rare (e.g. AB → B was observed 73 times, AB → A 3 times), and we lack replicates.
  - Some events might be prevented by the exact parameters in the system.
- The model is built to predict all possible trajectories (and succeeds in doing so). Is it just over-prediction?
- For the transitions from 3 to 2 species, there are 60 possible trajectories ; the model predicts 43 of them, and 26 of these are observed.
  - ⇒ The probability that all 26 observed transitions fall into the model purely by chance is  $(\frac{43}{60})^{26} \approx 6.10^{-4}$ .
  - For transitions from 4 to 3 species, 60 possible / 43 in the model / 19 observed ⇒ probability ≈  $4.10^{-4}$ .

### What is it useful for?

- **Parameter-free** model: it should be valid for any system with the same interaction network -- the exact trajectories will depend on parameters, but they should stay within the canvas of allowed transitions anyway.
- We trade the precision of predictions for their robustness.
- Still allows to draw conclusions: here, we can demonstrate that states reachable via bottom-up assembly may not be reachable via top-down assembly (e.g. BP).
- ... More generally, in trophic networks, the starting state appears critical for top-down assembly ! (While it matters little or not at all for competitive networks, see Serván & Allesina 2020.)
- Can be helpful for experimental design, as the model is easy to write in advance.
- Does not rely on hardy-measurable parameters : allows direct model/data analysis !
- Modeling the data allowed us to modify the trophic network postulated a priori, and to infer the presence of competition.
- NB: no stable state has been observed except trivial ones (single species or non-interacting species), but the ability of states to persist varies a lot (never more than 2 weeks for some, more than 20 for others).

# What is the ecological value of fragmented landscapes?

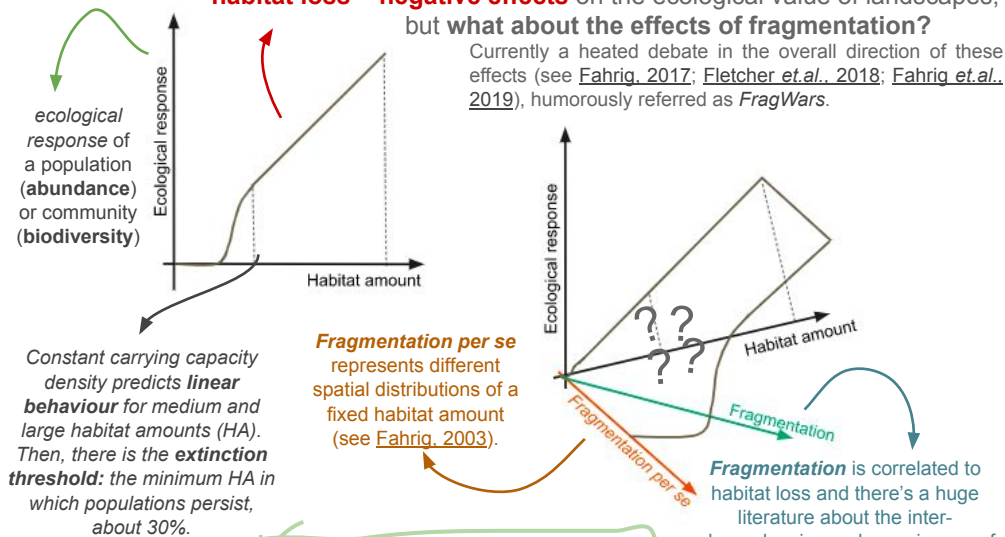
## Population dynamics in highly fragmented landscapes

Vítor Sudbrack<sup>\*1</sup>, Renato M. Coutinho<sup>2</sup>, Emílio Hernández-García<sup>3</sup>, Cristóbal López<sup>3</sup> & Roberto A. Kraenkel<sup>1</sup>  
<sup>1</sup>IFT-UNESP, São Paulo, Brazil. <sup>2</sup>CMCC-UFABC, São Paulo, Brazil. <sup>3</sup>IFISC-CSIC-UIB, Palma de Mallorca, Spain. \*vitorsudbrack@gmail.com

### Landscape ecology

**habitat loss = negative effects** on the ecological value of landscapes, but **what about the effects of fragmentation?**

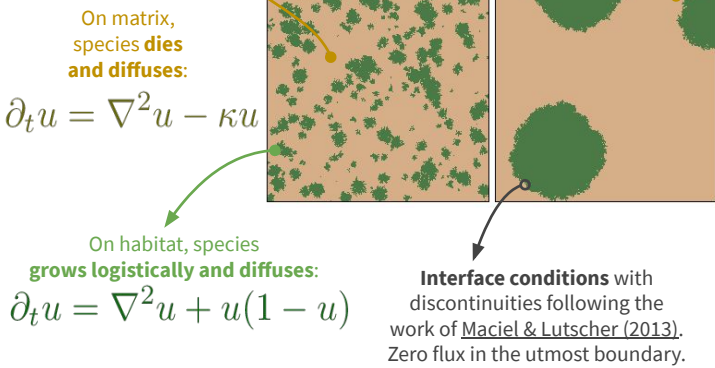
Currently a heated debate in the overall direction of these effects (see [Fahrig, 2017](#); [Fletcher et al., 2018](#); [Fahrig et al., 2019](#)), humorously referred as *FragWars*.



Can we use synthetic data to help elucidate and quantify the effects of fragmentation per se?

### Modelling

Two groups of artificial landscapes with fixed HA: **highly and slightly fragmented**

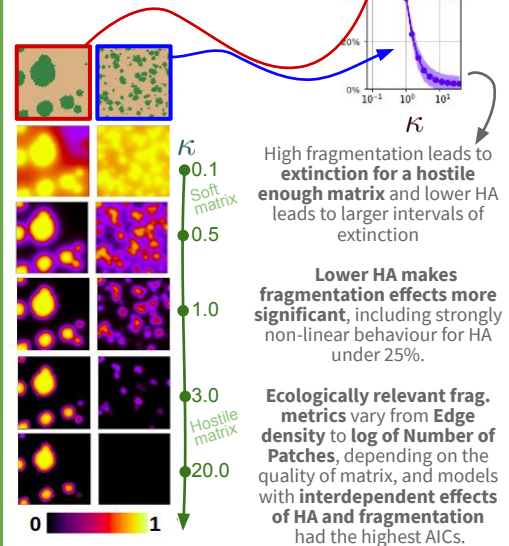


$\kappa$  is the only parameter of the model, it can be seen as the **hostility of matrix**

In order to **quantify the effects of fragmentation**, we tested **3 statistical models** with **7 different fragmentation metrics** using total pop. in the stationary state as response variable

### Single species abundance

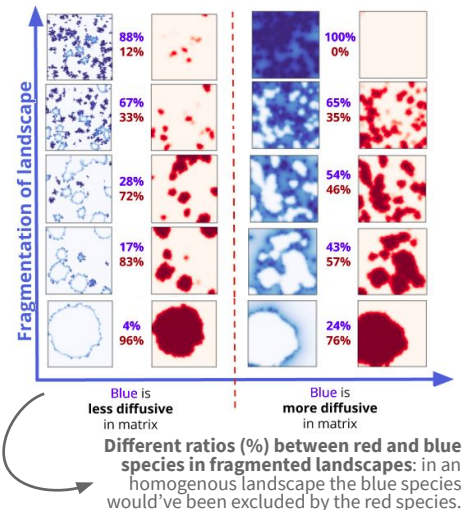
Population abundance as a function of matrix hostility averaged over the two groups of landscapes: **highly & slightly fragmented**. **Effects of fragmentation can be either good or bad, depending on the quality of matrix.**



### Two-species competition

The model can be easily adapted to multi-species models. In the case of in-habitat competition, we observe that considering different patch and matrix mobilities, the **degree of fragmentation is a key factor for coexistence**, both locally as well as in landscape.

We quantify the **mixing measures** of species spatial distributions in different landscapes and observe complex and non-negligible effects of fragmentation in the dynamics depending on a balance between **effects on competition and on mobility**.



Read more about this project at <https://vsudbrack.github.io/projects/frag>

SUPPORT OF



IFT - UNESP  
INSTITUTO DE FÍSICA TEÓRICA

unesp  
UNIVERSIDADE ESTADUAL PAULISTA  
"JÚLIO DE MESQUITA FILHO"



## Structuring and Optimization of an individual based model

Irina Lerner<sup>1</sup>

Carlos Eduardo Ferreira<sup>2</sup>, Flávia Maria Darcie Marquitti<sup>3</sup>

<sup>1</sup>Curso de Ciências Moleculares, University of São Paulo

<sup>2</sup>Instituto de Matemática e Estatística, University of São Paulo

<sup>3</sup>Instituto de Física Gleb Watghin, State University of Campinas

[irina.lerner@usp.br](mailto:irina.lerner@usp.br)

### Objectives

In the present work, we study speciation using an individual based model (IBM). We implement in the C programming language a model proposed by Aguiar *et al.*, (2009). A population is modeled as a genetic flow graph, with optimized algorithms for construction and search for connected components, which represent the species. At last, validation and efficiency tests is conducted.

### Methods

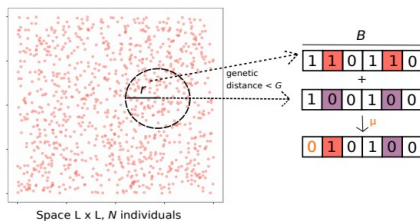


Figure 1:  $N$  individuals, arranged in a limited space, with binary genomes of size  $B$ . Each individual looks for a partner in an area of defined radius  $r$ . A pair mates if they are compatible (genetic distance  $< G$ ). There is a descendant, if they breed, whose genome is a combination of parental genomes with random mutations at a  $\mu$  rate.

Each individual is represented by a vertex of a graph, and there is an edge between two vertices if the individuals are compatible.

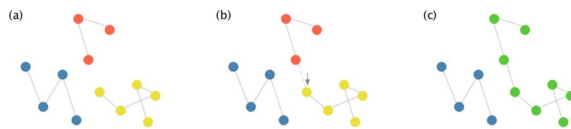


Figure 2: Example of a gene flow graph. There are several isolated connected components, which we will call species, represented in different colors.

To find the species (connected components) in the graph, we use depth-first search (DFS), in V0 and V1, and *Union-Find*, in V2 (Fig 3).

### Resultados

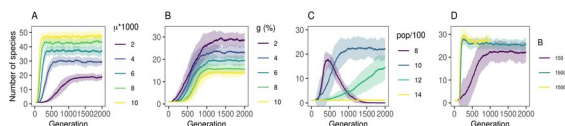


Figure 2: Lines represent the average number of species in 50 replicates. And the shadow, the standard deviation. In A, B, C and D only vary  $\mu$ ,  $G$ ,  $N$ ,  $B$ , respectively

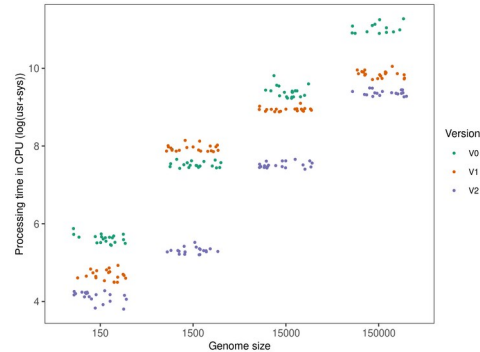


Figure 3: execution time of each implemented version of the program is compared in terms of CPU time, on a logarithmic scale. V0 is the version without optimizations, V1 is the version with genomes in linked lists. V2 is the version with the previous optimization and Union-Find as search algorithm.

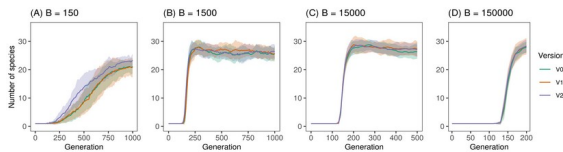


Figure 4: The lines represent the average number of species in 20 trials, in each version implemented. The shadow represents the standard deviation. All parameters, except the genome, are fixed. In (A)  $B = 150$ , (B)  $B = 1500$  (C)  $B = 15000$  (D)  $B = 150000$ .

### Conclusions

Based on figure 2, the number of species increases with the increase in  $\mu$  and  $B$ , and with the reduction in  $G$  and  $N$ , which is consistent with the trends of the model proposed by Derrida-Higgs and later implemented for the finite genome version by De Aguiar *et al.* (2009) and Costa *et al.* (2019).

We can see in Figure 3 that the optimization actually reduces the program execution time significantly, without changing the number of species pattern, for large genomes, as can be seen in Figure 4.

### References

De Aguiar, M. A. M., M. Baranger, E. Baptistini, L. Kaufman, and Y. Bar-Yam, 2009. Global patterns of speciation and diversity. *Nature* 460:384.

Costa, C. L., P. Lemos-Costa, F. M. Marquitti, L. D.Fernandes, M. F. Ramos, D. M. Schneider, A. B.Martins, and M. A. de Aguiar, 2019. Signatures of microevolutionary processes in phylogenetic pat-terns. *Systematic Biology* 68:131–144.



# Impact of the landscape heterogeneity on the spatial organization of a single-species population

V. Dornelas<sup>1,2</sup>, E. H. Colombo<sup>3</sup>, C. López<sup>3</sup>, E. Hernández-García<sup>3</sup> and C. Anteneodo<sup>1,4</sup>



<sup>1</sup> Department of Physics, PUC-Rio, Rio de Janeiro, Brazil, <sup>2</sup> ICTP-SAIFR & Institute of Theoretical Physics - UNESP  
<sup>3</sup> IFISC (CSIC-UIB), Campus Universitat Illes Balears, Palma de Mallorca, Spain, <sup>4</sup> Institute of Science and Technology for Complex Systems, Rio de Janeiro, Brazil



It is common to observe in nature the emergence of collective behavior in biological populations, such as pattern formation. In this work, we are interested in characterizing the distribution of a single-species population (such as some bacteria or vegetation), based on mathematical models that describe the spatio-temporal evolution of the density, governed by elementary processes, such as dispersion, growth, and nonlocal competition by resources. Using a generalization of the FKPP equation, we study the role that a heterogeneous environment has in the spatial organization of a population. We investigate the structures that emerge near the border from one environment to the other. We found that, depending on the shape of nonlocal interaction and other model parameters, three different profiles can emerge from the interface: *sustained oscillations*, *attenuated oscillations*, and *exponential decay* to a flat profile. We related the wavelength and the rate of decay of oscillations with the parameters of the interaction (characteristic length and form of decay with distance). We discussed how the heterogeneities of the environment allow access to information about the biological phenomena of the system, hidden in the homogeneous case, such as those that mediate competitive interactions.

## Mathematical model

We consider the following generalization of the one-dimensional FKPP equation, for the spatial distribution of single-species populations in a heterogeneous environment:

$$\partial_t \rho(x, t) = D \partial_{xx} \rho(x, t) + \Psi(x) \rho(x, t) - b \rho(x, t) [\gamma * \rho](x, t)$$

where:

- $D$  → Diffusion coefficient
- $\Psi(x)$  → Spatially-dependent reproduction rate
- $\gamma(x)$  → Influence function of nonlocal competition

### Interaction kernel

The mathematical model takes into account that individuals in the population compete for resources with all neighbors within an  $\ell$  distance, and this interaction is mediated by an influence function that gives by

$$\gamma_\ell(x) = \frac{2-q}{2\ell} [1 - (1-q)|x|/\ell]_+^{1/(1-q)}$$

## Homogeneous landscapes

For a homogeneous landscape,  $\Psi(x) = a$ , from the linear stability analysis, we find the mode growth rate

$$\lambda(k) = -Dk^2 - a\tilde{\gamma}(k),$$

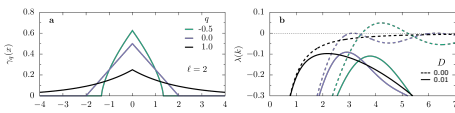


Figure 1: Interaction kernel (a) and mode stability in a homogeneous medium

- If  $\lambda < 0$ , in the long-time limit, the population distribution  $\rho(x)$  will be flat (homogeneous distribution).
- If  $\lambda(k) > 0$ , there are unstable modes, and stationary sustained oscillations will be produced with a characteristic mode  $k^*$  (the maximum of  $\lambda$ ).

## Heterogeneous landscapes

The heterogeneous environment is introduced by assuming that the growth rate can be written as spatial variations around a reference level:

$$\Psi(x) = a + \psi(x)$$

We focus on sharp spatial changes in the environmental conditions.

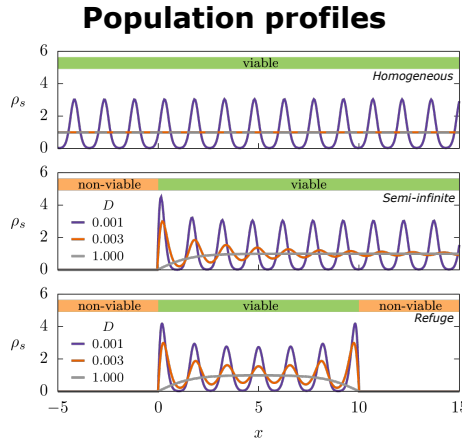
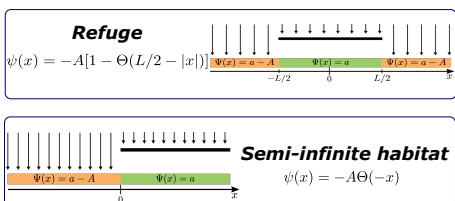


Figure 2: Population distribution in three types of environment. Even when the steady-state is uniform in case (a), decaying oscillations can emerge in (b)-(c). The parameters for the kernel are  $q = -0.5$  and  $\ell = 2$ , and  $A \rightarrow \infty$  for panels (b) and (c).

- *sustained oscillations* (or spatial patterns, without amplitude decay);
- *decaying oscillations* (with decreasing amplitude from the interface);
- *exponential decay* towards a flat profile.

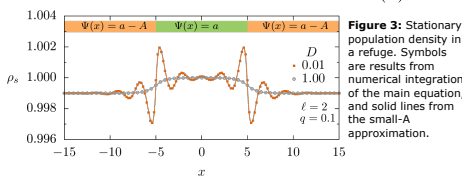
## Refuge

### Approximate analytical solution

In the limit of weak heterogeneity  $|\psi(x)|/a \ll 1$

- Find the nontrivial homogeneous solution:  $\rho_0 = a/b$
- Assuming a small perturbation around the  $\rho_0$ :  $\rho(x, t) = \rho_0 + \varepsilon(x, t)$
- Fourier transforming the stationary case:  $\tilde{\rho}_s(k) = 2\pi\rho_0\delta(k) + \frac{\rho_0\tilde{\psi}(k)}{-\lambda(k)}$
- Anti-transforming Fourier:

$$\rho_s(x) = \rho_0 + \varepsilon_s(x) = \rho_0 + \mathcal{F}^{-1} \left( \frac{\rho_0\tilde{\psi}(k)}{-\lambda(k)} \right)$$



## Semi-infinite habitat

### Characterization of stationary profiles

For each steady distribution attained at long times, we measure the wavelength and the decay length, as depicted:

- Wavelength  $2\pi/\bar{k}$
- Decay length  $\bar{x}$

## Theoretical framework

**Theoretical 1:** The predictions of the oscillatory regime are based on mode linear stability analysis, relating the poles of  $1/\lambda(k)$ , given by  $k = \pm k_r + ik_i$ , and the oscillatory parameters by

$$\bar{k} = k_r \quad 1/\bar{x} = k_i$$

|                        |                   |
|------------------------|-------------------|
| Exponential decay      | $k_r = 0$         |
| Decaying oscillations  | $k_r, k_i \neq 0$ |
| Sustained oscillations | $k_i = 0$         |

**Theoretical 2:** Analogy between the solution of the steady-state density distribution and the forced linear oscillator, described by

$$\ddot{y} + 2\zeta k_0 \dot{y} + k_0^2 y = k_0^2 \Theta(x)$$

### Phase diagram

In Fig. 4a, for each point in the grid, the type of regime was determined based on the values of  $2\pi/\bar{k}$  and  $\bar{x}$  that characterize the profiles. Fig. 4b displays  $\bar{k}$  and  $\bar{x}$  as a function of  $q$ , for a fixed value of the diffusion coefficient, corresponding to a horizontal cut in (a).

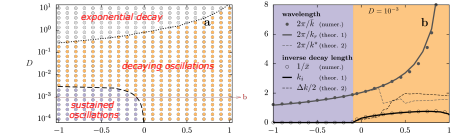
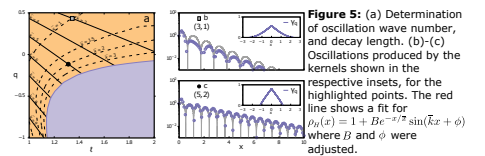


Figure 4: Phase diagram and characteristics of the stationary profiles as a function of the diffusion coefficient  $D$  and  $q$ , in the semi-infinite habitat.

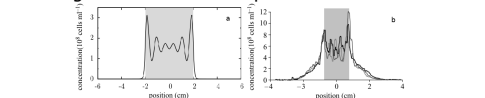
## Inferring information about the interactions

Using the theoretical estimates, we plot in Fig. 5a the contour lines for fixed wavelengths and decay lengths. If oscillations with specific values of  $\bar{k}$  and  $\bar{x}$  are observed in a population (black circles and gray squares in Fig. 5b-c), then, we can extract the interaction length  $\ell$  and the shape exponent  $q$ , from the  $(\ell, q) \leftrightarrow (\bar{k}, \bar{x})$  mapping.



## Comparison with experimental data

The spatial organization is qualitatively similar to the case experimentally investigated by N. Perry, although it needs to incorporate other elements.



### Summary

- We have studied the non-local FKPP equation in the presence of heterogeneous environments.
- We have identified three types of spatial structures close to a discontinuity of the environment.
- We provide theoretical predictions of the profile based on mode linear stability analysis.
- The sharp heterogeneities reveal information on the interaction scales, that are otherwise hidden.

Reference:



Acknowledgment:





# Predicting collapse of networked systems without knowing the network

Leonhard Horstmeyer<sup>1,2</sup>, Tuan Minh Pham<sup>1,2</sup>, Jan Korbel<sup>1,2</sup>, Stefan Thurner<sup>1,2,3,4</sup>

<sup>1</sup>Section for the Science of Complex Systems, CeMSIS, Medical University of Vienna, Spitalgasse 23, A-1090, Vienna, Austria  
<sup>2</sup>Complexity Science Hub Vienna, Josefstädterstrasse 39, A-1090 Vienna, Austria  
<sup>3</sup>Santa Fe Institute, 1399 Hyde Park Road, Santa Fe, NM 87501, USA; <sup>4</sup>IIASA, Schlossplatz 1, 2361 Laxenburg, Austria

## Abstract

The collapse of ecosystems, the extinction of species or the breakdown of banking networks usually hinges on topological properties of the underlying interaction network. Without structural information it seems impossible to say whether the network is in the critical state of an impending collapse. We show that for a large class of dynamical systems with coupled node-link dynamics, a temporal network with a *single* directed cycle can exhibit the *quantization* of the state vector. We use this phenomenon as an indicator of collapse in many complex systems.

## Theorem (Eigenvector Quantization [1])

Let  $M^t$  be a binary temporal matrix with entries  $M_{ij}^t \in \{0,1\}$  and diagonal entries  $M_{ii}^t = 0$  for all  $i \in \{1, \dots, N\}$ . Let  $G^t$  be the directed network with the adjacency matrix  $M^t$ . For any fixed instance of  $M^t$ , let  $X(\tau) = (X_1(\tau), \dots, X_N(\tau))$  be an  $N$ -dimensional state vector, whose components  $X_i(\tau)$  evolve according to

$$\frac{d}{d\tau} X_i = \sum_{j=1}^N M_{ij}^t X_j - \Phi X_i. \quad (1)$$

Then the following holds for  $x^t$  defined as  $x_i(\tau) = X_i(\tau) / \sum_j X_j(\tau)$ :

- (i) **Convergence:** For any initial condition  $\mathbf{x}(0)$  except a set of points of Lebesgue-measure zero  $\mathbf{x}(\tau)$  converges to a stable fixed point  $\mathbf{x}^t := \lim_{\tau \rightarrow \infty} \mathbf{x}(\tau)$  that is a non-negative eigenvector of  $M^t$ .
- (ii) **Eigenvector Quantization:** Suppose  $G^t$  contains a cycle, and there is no node that is part of more than one cycle. Then any component  $x_i^t > 0$  at time  $t$  can be expressed via the number of directed paths  $n_i \in \mathbb{N}$  that leading from cycle-nodes to  $i$  as

$$x_i^t = n_i x_{\min}^t, \quad (2)$$

where  $x_{\min}^t$  is the minimal component (cycle-nodes).

## Application: Expected time to collapse $T$ in the Jain-Krishna model [2]

The model includes a fast dynamics of the nodes given by Eq. (1) on a fixed network, and a slow dynamics of the graph. The dynamics is iterated via 3 steps: i) for fixed  $M$ , Eq. (1) is integrated to find  $\mathbf{x}$ ; ii) the graph then is updated from  $M$  to  $M'$  by eliminating one of the least fit species and creating a new species, say  $i$ , with a small abundance. The species  $i$  is randomly connected to preexisting species  $j$  by in-links to ( $M_{ij}^t = 1$ ), and out-links from ( $M_{ji}^t = 1$ )  $i$ , both with the same probability  $m/(N-1)$ ; iii) Return to step i) with  $M = M'$ .

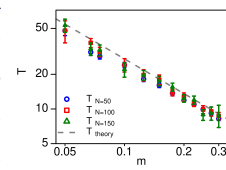


Figure 1: Expected time to collapse  $T$  as a function of the average connectivity  $m$ . The total number of species  $N = 50, 100, 150$ .

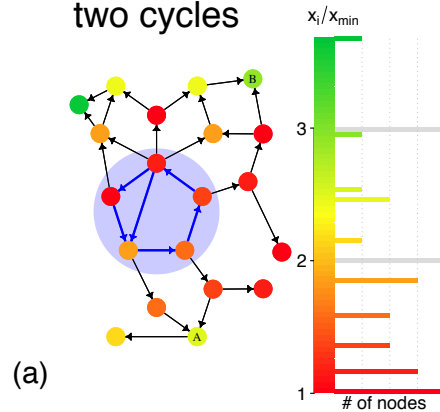
The precursor based on Eigenvector Quantization predicts

$$T = e/m$$

## Contact Information

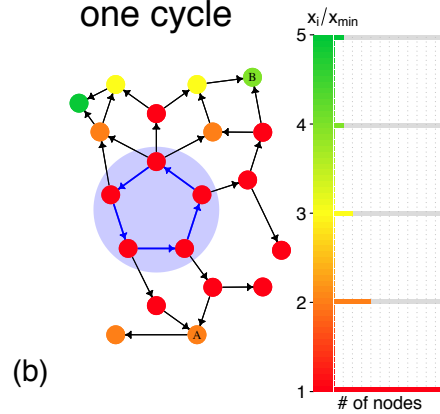
tuan.pham@meduniwien.ac.at

## two cycles



(a)

## one cycle



(b)

Figure 2: Graphical demonstration of the Theorem. The directed networks  $M^t$  at two different time  $t$  is shown. In (a)  $M^t$  contains two cycles (a) and in (b) – one cycle. Cycles are in the shaded area. The color of the nodes indicates the state  $x_i^t$  in units of the minimal value  $x_{\min}^t$ . The histograms show the number of nodes in a given state. The quantization of states is seen in (b), but not in (a). Since  $A$  can be reached via two paths from the cycle, while node  $B$  can be reached by four, the state  $x_A/x_{\min} = 2$  and  $x_B/x_{\min} = 4$  in the single cycle network (b). The number of paths no longer coincides with the states in (a).

## References

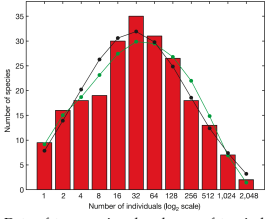
- [1] L. Horstmeyer, T. M. Pham, J. Korbel, and S. Thurner. Predicting collapse of adaptive networked systems without knowing the network. *Scientific Reports*, 10:1223, 2020. doi: 10.1038/s41598-020-57751-y.
- [2] S. Jain and S. Krishna. Autocatalytic sets and the growth of complexity in an evolutionary model. *Phys. Rev. Lett.*, 81:5684–5687, Dec 1998. ISSN 0031-9007. doi: 10.1103/PhysRevLett.81.5684.

## Patterns of speciation and diversification in a model with selection over mito-nuclear compatibility

Débora Princepe<sup>\*1,2</sup>, Marcus A. M. de Aguiar<sup>1</sup>, and Joshua B. Plotkin<sup>2</sup>

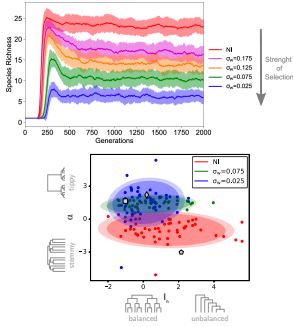
1. Instituto de Física "Gleb Wataghin", Universidade Estadual de Campinas – Campinas, SP, Brazil  
 2. Department of Biology, University of Pennsylvania – Philadelphia, PA, United States

Understanding the origin and maintenance of biodiversity is one of the main questions in ecology. The neutral theory succeeded in explaining patterns of species abundances distributions (SADs), which are similarly obtained with niche models, but there are features that remain unclear, such as the impact of the speciation rate and of species lifetimes in those distributions.



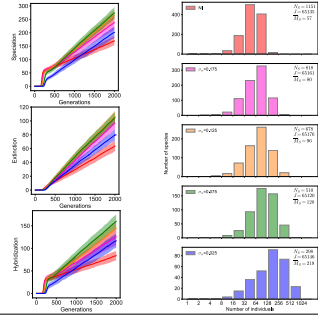
Data of tree species abundances of tropical forests in Panama are very explored in the literature and well fit by the zero-sum multinomial distribution derived from Hubbell's unified neutral theory of biodiversity [1,2].

Using an individual-based model, we explored the impact of selection over the individual mito-nuclear compatibility in the speciation process of populations in parapatry, analyzing the signatures left in the resulting phylogenies and in genetic correlations within and between species.



Our previous results on the model with mito-nuclear coevolution [3].

Here we show our first analyzes of the effect of selection on species abundances and lifetimes in this model, unveiling how abundances distributions can be connected with species history, ages and the different processes guiding diversification.



REFERENCES

1. S. P. Hubbell, The Unified Neutral Theory of Biodiversity and Biogeography (Princeton Univ. Press, Princeton, 2001).
2. I. Volkov, J. R. Banavar, S. P. Hubbell, A. Maritan, Nature 424, 1035 (2003).
3. D. Princepe, M. A. M. De Aguiar, Systematic Biology 70, 133 (2021).